ISSN 1070-3284, Russian Journal of Coordination Chemistry, 2022, Vol. 48, No. 10, pp. 608–614. © Pleiades Publishing, Ltd., 2022.
Russian Text © The Author(s), 2022, published in Koordinatsionnaya Khimiya, 2022, Vol. 48, No. 10, pp. 590–597.

Dedicated to Academician Yu.A. Zolotov in the year of his 90th birthday

Zinc Pentafluorobenzoate $[Zn_2(H_2O)(C_6F_5COO)_4(Py)_4]$: Synthesis, Structure, and Thermodynamic Characteristics

I. P. Malkerova[a], D. B. Kayumova[a], E. V. Belova[a], M. A. Shmelev[a], A. A. Sidorov[a], and A. S. Alikhanyan[a, *]

[a] *Kurnakov Institute of General and Inorganic Chemistry, Russian Academy of Sciences, Moscow, 119992 Russia*

**e-mail: alikhan@igic.ras.ru*

Received March 15, 2022; revised April 14, 2022; accepted April 16, 2022

Abstract—The reaction of zinc pentafluorobenzoate $[Zn(H_2O)(C_6F_5COO)_2]_n$ with a pyridine excess (Py, ratio Zn : Py = 1 : 4) affords crystals of complex $[Zn_2(H_2O)(C_6F_5COO)_4(Py)_4]$ (**I**). The crystal packing of complex **I** is stabilized by numerous intra- and intermolecular interactions π...π, O...H, F...π, C–H...F, and C–H...O. The compound is characterized by the data of X-ray diffraction (XRD) (CIF file CCDC no. 2157445), IR spectroscopy, C,H,N elemental analysis, and phase XRD analysis. The vaporization of $[Zn_2(H_2O)(C_6F_5COO)_4(Py)_4]$ is studied by the Knudsen effusion method with mass spectral analysis of the gas phase. This process is found to proceed in three stages with the consecutive transition of pyridine molecules to the vapor, partial hydrolysis, and congruent sublimation of zinc pentafluorobenzoate to form free molecules of $Zn(C_6F_5)_2$ and CO_2. The absolute partial pressures of saturated vapor and standard enthalpies of formation are calculated: $\Delta_f H^\circ_{298}(Zn(C_6F_5COO)_2, s) \le -2634.1 \pm 32.2$ kJ/mol and $\Delta_f H^\circ_{298}(Zn(C_6F_5)_2, g) \le -1422.6 \pm 31.3$ kJ/mol.

Keywords: XRD, phase XRD, mass spectrometry, synthesis, structure, zinc pentafluorobenzoate, noncovalent interactions, thermodynamics, vaporization, standard enthalpies of formation

DOI: 10.1134/S1070328422100037

INTRODUCTION

Thin indium–tin oxide (ITO) films demanded by modern industry are expensive, which impels to search for cheaper analogs. Among other materials, zinc oxide [1–4] and fluorine-doped zinc oxide (FZO) [2, 3] were proposed as such analogs. Zinc oxide films and nanoparticles prepared by various methods found use in photocatalysis [4], sensor manufacturing [5–9], and biomedicine [10, 11]. As compared to zinc oxide, FZO has a number of advantages: an anomalously high linear electrooptical effect [12] and more uniform cathode luminescence properties [13], which makes it still more attractive for commercial use.

Diverse combinations of precursors (sources of ZnO and fluorinating agents) are often used for the preparation of FZO, for example, diethylzinc and hexafluoropropene [5] or zinc acetate and ammonium fluoride [14]. The possibility of preparing zinc oxide films with the fluorine content about 1.2% from fluorinated zinc ketoiminates was demonstrated [15]. The use of these precursors has several advantages: they are volatile, do not require oxygen during deposition, undergo deposition at temperatures of the precursor and support of 250 and 400°C, respectively, and have a very low carbon contamination in the bulk. British researchers [16] prepared the fluorine-doped tin oxide films from fluorine-containing carboxylates but failed to obtain FZO using this method [17]. It seemed interesting to study the vaporization of zinc pentafluorobenzoate to determine the gas phase composition and thermodynamic characteristics.

EXPERIMENTAL

All procedures on the synthesis of complex $[Zn_2(H_2O)(C_6F_5COO)_4(Py)_4]$ (**I**) were carried out in air using commercially available pyridine (Py, ≥99%, Sigma-Aldrich) and ethanol (96%). Compound $[Zn(H_2O)(C_6F_5COO)_2]_n$ was synthesized using a known procedure [18].

The IR spectra of compound **I** were recorded on a Spectrum 65 FT-IR spectrometer (PerkinElmer) by the attenuated total reflection (ATR) method in a frequency range of 4000–400 cm^{-1}. Elemental analysis was carried out on a EuroEA 3000 CHNS analyzer (EuroVector).

XRD of a single crystal of the compound was carried out on a Bruker D8 Venture diffractometer equipped with a CCD detector (MoK_α, $\lambda = 0.71073$ Å, graphite monochromator) [19]. A semiempirical absorption correction was applied using the SADABS program [20]. The structure was solved by direct methods and refined by full-matrix least squares in the anisotropic approximation for all non-hydrogen atoms. The positions of hydrogen atomes were generated geometrically. All hydrogen atoms were refined in the isotropic approximation by the riding model. The calculations were performed using the SHELX software [21] and OLEX2 [22]. The geometry of a polyhedron of the metal atom was determined using the SHAPE 2.1 program [23, 24].

The coordinates of atoms and other parameters of the compound were deposited with the Cambridge Crystallographic Data Centre (CIF file CCDC no. 2157445; deposit@ccdc.cam.ac.uk or http://www.ccdc.cam.ac.uk/data_request/cif).

The crystallographic data and structure refinement details for complex **I** at $T = 100(2)$ K are as follows: $C_{48}H_{22}N_4O_9F_{20}Zn_2$, $M_w = 1309.43$ g/mol, monoclinic crystal system, space group $C2/c$, $a = 15.255(3)$, $b = 14.483(3)$, $c = 23.583(4)$ Å, $\alpha = 90°$, $\beta = 108.273(15)°$, $\gamma = 90°$, $V = 4947.9(17)$ Å^3, $Z = 4$, $\rho_{calc} = 1.758$ g cm^{-3}, $\mu = 1.106$ mm^{-1}, $1.988° \le \theta \le 30.506°$, segment of sphere $-21 \le h \le 20$, $-20 \le k \le 18$, $-28 \le l \le 33$, $T_{min}/T_{max} = 0.725/0.811$, 37175 measured reflections, 7525 independent reflections, 6149 reflections with $I > 2.0\sigma(I)$, $R_{int} = 0.0491$, GOOF = 1.033, R_1 ($I > 2\sigma(I)$) = 0.0325, wR_2 ($I > 2\sigma(I)$) = 0.0720, R_1 (all data) = 0.0462, wR_2 (all data) = 0.0764, $\Delta\rho_{min}/\Delta\rho_{max}$, e Å^{-3} = –0.462/0.387.

The phase XRD analysis of the sample was carried out on a Bruker D8 Advance diffractometer (CuK_α, $\lambda = 1.54060$ Å, Ni filter, LYNXEYE detector, reflection geometry). The detection increment was 0.02° 2θ, and the detection range was 5°–40° 2θ. The experimental and theoretical XRD patterns were compared using the TOPAS 4 software.

Synthesis of $[Zn_2(H_2O)(C_6F_5COO)_4(Py)_4]$ (I). A weighed sample of compound $[Zn(H_2O)(C_6F_5COO)_2]_n$ (0.100 g, 0.198 mmol) was dissolved in EtOH (15 mL) at 70°C for 20 min, and pyridine (66 μL, 0.792 mmol, Zn : Py = 1 : 4) was added to the hot solution. The resulting colorless solution was hold at 70°C in a closed vial. Colorless crystals suitable for XRD formed in 3 days were separated from the mother liquor by decantation and washed with cold EtOH (T = ~5°C). The yield of compound **I** was 0.093 g (72.1% based on compound $[Zn(H_2O)(C_6F_5COO)_2]_n$).

For $C_{48}H_{22}N_4O_9F_{20}Zn_2$			
Anal. calcd., %	C, 44.0	H, 1.7	N, 4.3
Found, %:	C, 44.2	H, 1.4	N, 4.0

IR (ATR; ν, cm^{-1}): 3071 w, 2631 w, 1662 s, 1600 s, 1589 s, 1562 m, 1522 s, 1491 s, 1448 s, 1381 s, 1291 s, 1225 m, 1155 s, 1140 m, 1100 s, 1072 s, 1041 s, 991 s, 929 s, 918 m, 863 m, 829 s, 761 s, 733 s, 698 s, 685 s, 650 m, 632 s, 578 s, 509 m, 480 m, 453 m, 420 s.

RESULTS AND DISCUSSION

We have previously developed the following procedure for the synthesis of *d*- and 4*f*-metal pentafluorobenzoates: a stoichiometric amount of pentafluorobenzoic acid was added to freshly precipitated hydroxide of the corresponding metal in water, which was prepared in situ, and the mixture was stirred to the complete dissolution of the precipitate [25, 26]. The obtained solutions were stored at room temperature and slow evaporation to the formation of crystals. However, in the case of zinc, this approach did not give crystals of zinc pentafluorobenzoate suitable for XRD, because only a white amorphous precipitate was formed.

We proposed a new procedure for the synthesis of zinc pentafluorobenzoate based on the exchange reaction between zinc nitrate and pentafluorobenzoic acid potassium salt in ethanol. As a result, the crystals of new compound $[Zn(H_2O)(C_6F_5COO)_2]_n$ were isolated [18]. An advantage of this procedure is a simplicity of the experiment and a high (close to100%) yield of the target product. The task of using the synthesized zinc pentafluorobenzoate was complicated by the fact that this compound, in our opinion, is not appropriate for the purposes indicated above because of a high water content sufficient to provide hydrolysis and low volatility of the products. It was shown that the reaction of $[Zn(H_2O)(C_6F_5COO)_2]_n$ with pyridine (ratio Zn : Py = 1 : 4) afforded binuclear molecular complex $[Zn_2(H_2O)(C_6F_5COO)_4(Py)_4]$ (Fig. 1) containing a halved amount of water.

The structure of the synthesized compound was determined by XRD, and the phase purity and composition of the complex were confirmed by phase XRD (Fig. 2) and elemental analysis data.

According to the XRD data, compound **I** crystallizes in the monoclinic space group $C2/c$ with the inversion center between the zinc ions. In the structure of complex **I**, the metal ions are linked by two bridging $C_6F_5COO^-$ anions and bridging water molecule (Zn...Zn 3.679(1) Å; Zn–O(μ^2-C_6F_5COO) 2.089(1), 2.109(1) Å; Zn–O(μ^2-H_2O) 2.142(1) Å). Each metal center builds up its environment to an octahedron (ZnN_2O_4, $S_Q(Zn) = 0.107$ [23, 24] by the coordination of the O atoms of the monodentate-bound $C_6F_5COO^-$ anion and two pyridine molecules (Zn–O(κ^1-C_6F_5COO) 2.162(1); Zn–N(Py) 2.116(1), 2.139(1) Å).

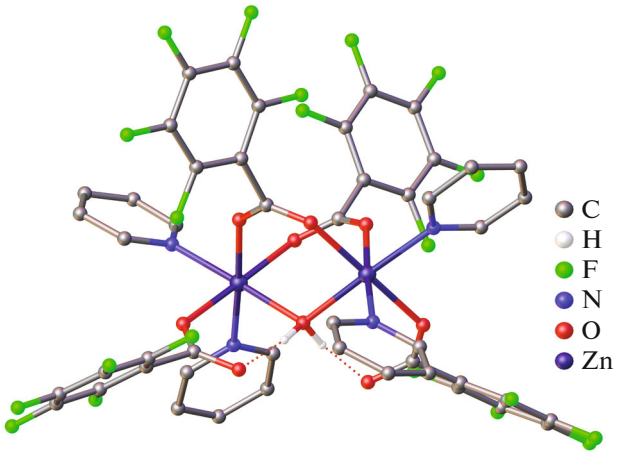

Fig. 1. Structure of complex **I**. Hydrogen atoms in the pyridine molecule are omitted.

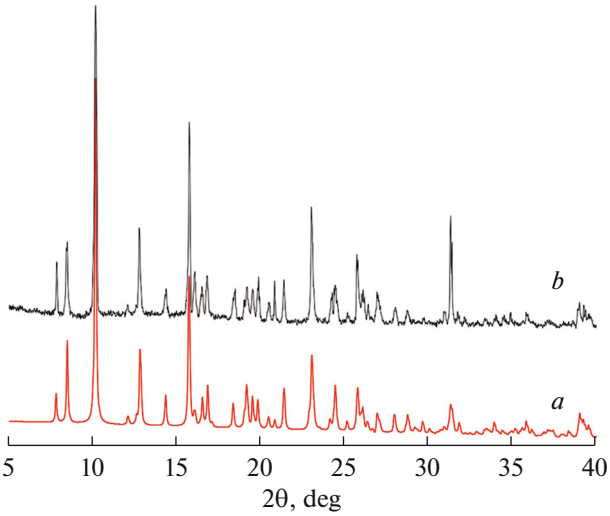

Fig. 2. Comparison of the (*a*) calculated and (*b*) experimental XRD patterns for compound **I**.

Compounds $[M_2^{2+}(H_2O)(RCOO^-)_4(Py)_4]$ were earlier obtained for a series of transition metals (Ni [27], Mn [28], Co [29], Cu [30]), whereas this is the first example of such a complex for the zinc ion, since the formation of mononuclear or binuclear complexes $[Zn(RCOO)_2(Py)_2]$ or $[Zn_2(RCOO)_4(Py)_2]$ is more typical of zinc [31–37].

The coordinated water molecule forms intramolecular hydrogen bonds with the O atoms of two monodentate-bound $C_6F_5COO^-$ anions (O(1*w*)–O(2) 2.572(1) Å, O(1*w*)H(1*w*)O(2) 169.2°) (Fig. 1).

The packing of the complex exhibits a close to parallel orientation of the C_6F_5 and Py aromatic moieties of the adjacent molecules (angle between the planes, shortest distance between the planes, and distance between centroids of the pentafluorobenzoate anions are 0.04°, 3.292 and 3.628 Å, respectively; and those between the pyridine molecules are 3.57°, 3.495, and 3.641 Å, respectively (Fig. 3)). This indicates the formation of π–π interactions between them. An additional stabilization of the crystal structure due to C–H...F, C–H...O, and C–F...π interactions with the formation of a supramolecular structure is also observed (C–H...F 2.46–2.50, C...F 3.050–3.179 Å, angle C–H...F 120°–129° for interactions C–H...F; C–H...O 2.46–2.59, C...O 3.026–3.312 Å, angle C–H...O 113°–150° for interactions C–H...O; C–F...π 3.17–3.51 Å for interactions C–F... π).

An analogous stabilization of crystal packing was observed for the cadmium pentafluorobenzoate complexes and heterometallic compounds {Cd-Ln}, where noncovalent interactions resulted in a significant distortion of the geometry of the complexes and formation of polymeric structures of new types [26, 38].

The sublimation (vaporization) of the complex was studied on an MS 1301 instrument by the Knudsen effusion method with mass spectral analysis of the gas phase composition in a temperature range of 300–575 K. The procedure and instrument were described in detail [39]. Molybdenum Knudsen effusion cells with the ratio of the evaporation surface area to the effusion surface area equal to ~600 were used. The temperature was measured with a Pt/Pt-Rh thermocouple and maintained constant with an accuracy of ±1°.

The mass spectra of the gas phase above the synthesized compound at different times and temperatures of experiment are given in Table 1. An analysis of the data showed that the vaporization of the complex can be described by three consecutive stages. Pyridine sublimes at the first stage (1) that starts at room temperature and occurs to 80–100°C. Then the partial hydrolysis of the complex with the transition of pentafluorobenzoic acid to the gas phase is observed in a temperature range of 150–230°C (2). After the end of hydrolysis, the sublimation of the remained weighed sample of zinc pentafluorobenzoate begins to occur noticeably at a higher temperature (3).

$$Zn(C_6F_5COO)_2\cdot 0.5H_2O\cdot 2Py(s) \rightarrow Zn(C_6F_5COO)_2\cdot 0.5H_2O(s) + 2Py(g), \quad (1)$$

$$4[Zn(C_6F_5COO)_2\cdot 0.5H_2O](s) \rightarrow 3Zn(C_6F_5COO)_2(s) + Zn(OH)_2(s) + 2C_6F_5COOH(g), \quad (2)$$

$$Zn(C_6F_5COO)_2(s) \rightarrow Zn(C_6F_5)_2(g) + 2CO_2(g). \quad (3)$$

As can be seen from Table 1, almost no signals corresponding to pyridine molecules are observed in the mass spectrum of the gas phase. This can be explained by a weak interaction of the complex with pyridine, which transfers to the gas phase at room temperature yet before the beginning of measurements. After the

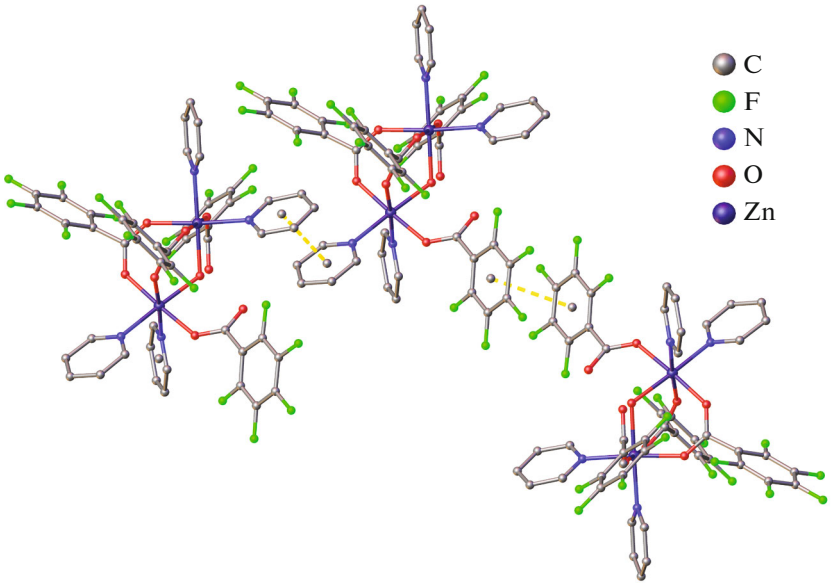

Fig. 3. Fragment of the crystal packing of complex **I** (π–π interactions are shown by dash).

end of the experiment, a minor amount of zinc oxide, which was formed by the decomposition of zinc hydroxide at the second stage of vaporization, remained in the effusion chamber.

Several experiments on the complete sublimation of the pyridine complex were carried out to determine the absolute partial pressures of the gas phase components and character of vaporization of the zinc pentafluorobenzoate phase. The result of one of the experiments is presented in Fig. 4, where only the second ($T = 446$ K) and third ($T = 503$ K) vaporization stages are shown for the reason indicated above. The initial monotonically decreasing intensities of the ion currents correspond to molecules of the acid formed upon hydrolysis at the second stage of vaporization. The subsequent constant intensities of the main ion currents correspond to the congruent sublimation of the $Zn(C_6F_5COO)_2$ phase. An analysis of the ionization efficiency of the ions in the mass spectrum showed that the saturated vapor consisted mainly of $Zn(C_6F_5)_2$ and CO_2 molecules. We failed to determine the nature of the $C_{12}F_{10}^+$ ion because of its low intensity in the mass spectrum, but this is likely a fission or rearrangement ion. Thus, the vaporization of zinc pentafluorobenzoate can be presented by reaction (3).

Table 1. Mass spectra of the gas phase above complex **I** ($U_{ioniz} = 70$ V)

m/z	Ion	*I*, rel. units		
		$T = 423$ K	$T = 446$ K	$T = 503$ K
		1st stage	2nd stage	3rd stage
79	Py^+	67	3	
167	$C_6F_5^+$	100	100	
192	$C_6F_4COO^+$	3	10	2.5
211	$C_6F_5COO^+$	3	8	0.25
64	$^{64}Zn^+$			20
230	$ZnC_6F_5^+$			70
249	$ZnFC_6F_5^+$			90
334	$C_{12}F_{10}^+$			4
396	$Zn(C_6F_5)_2^+$			100

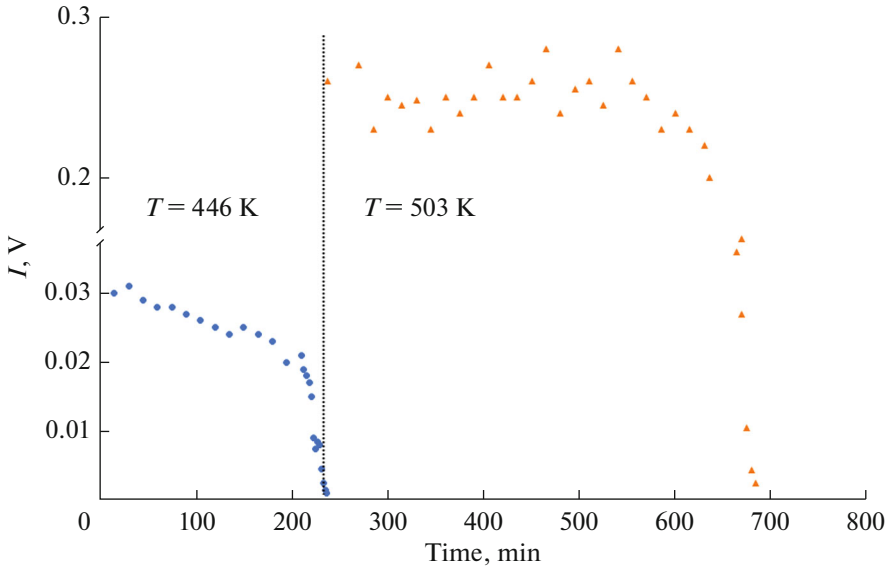

Fig. 4. Full sublimation isotherm for the known weighed sample of complex **I**. The second ($T = 446$ K) and third ($T = 503$ K) stages corresponding to the vaporization of acid C_6F_5COOH formed during hydrolysis and congruent sublimation of the $Zn(C_6F_5COO)_2$ phase, respectively, are shown.

The pressure of pyridine vapors was not calculated for the first stage of vaporization of the complex, because the corresponding ion current intensities cannot precisely be measured at the beginning of the experiment. The partial pressure of pentafluorodiphenylzinc during the congruent sublimation of zinc pentafluorobenzoate was calculated by the Hertz–Knudsen equation in the form

$$q_{Zn(C_6F_5)_2} = S_{eff}\left(\frac{M_{Zn(C_6F_5)_2}}{2\pi RT}\right)^{0.5}\int_{t_1}^{t_2} p_{Zn(C_6F_5)_2}dt$$

$$= k_i S_{eff}\left(\frac{M_{Zn(C_6F_5)_2}T}{2\pi R}\right)^{0.5}\int_{t_1}^{t_2} I_{Zn(C_6F_5)_2}dt$$

and the main equation of mass spectrometry

$$p_i = k_i I_i T,$$

where q_i is the weight of the complex evaporated in the form of $Zn(C_6F_5)_2$ molecules, S_{eff} is the effective effusion surface area, M_i is the molar mass of the ith component, T is temperature, p_i is the partial pressure of the ith component, t_1 (t_2) is the time of the onset (end) of congruent sublimation, k_i is the sensitivity coefficient for the ith component, I_i is the total ion current formed upon the ionization of the ith component.

The weight of the sample evaporated only in the form of pentafluorodiphenylzinc was calculated according to the stoichiometric formula of the synthesized complex $Zn(C_6F_5COO)_2{\cdot}0.5H_2O{\cdot}2Py$, weight of the nonvolatile ZnO residue in the effusion chamber (formed due to the hydrolysis of $Zn(C_6F_5COO)_2{\cdot}0.5H_2O$), thermal dissociation of zinc hydroxide (see reaction (2)), and congruent sublimation of zinc pentafluorobenzoate. The calculation results are given in Table 2. The partial pressure of carbon dioxide under the effusion experiment conditions was determined by the equation

$$2 = \frac{p_{CO_2}}{\sqrt{M_{CO_2}}} : \frac{p_{(C_6F_5)_2}}{\sqrt{M_{(C_6F_5)_2}}}.$$

The partial pressures corresponding to the total pressure minimum during zinc pentafluorobenzoate sublimation under the closed volume conditions are also listed in Table 2.

The standard enthalpy of congruent sublimation of zinc pentafluorobenzoate (3) was determined according to the second law of thermodynamics by the study of the temperature dependence of the equilibrium constant $k_p^* = (I_i T)^3$ written (by act of congruent sublimation) via different ion currents containing zinc atoms using the Van't Hoff equation by least squares (Table 3).

The average enthalpy of congruent sublimation of zinc pentafluorobenzoate turned out to be $\Delta_r H_T^\circ = 424.5 \pm 11.3$ kJ/mol.

To estimate the standard enthalpy of formation of pentafluorodiphenylzinc $Zn(C_6F_5)_2$, the dissociative ionization processes were studied for this complex and the energy of formation of the Zn^+ ion was determined (EA = 14.2 ± 0.3 V). The ionization energy EI of mercury atoms equal to 10.44 eV [40] was used as standard when determining the energy of formation. Accepting

Table 2. Partial pressures (Pa) of the saturated vapor components at $T = 503$ K

Phase	Sublimation conditions	Pressure		
		$p_{Zn(C_6F_5)_2}$	p_{CO_2}	p_{tot}
$Zn(C_6F_5COO)_2$	Knudsen	3.16×10^{-2}	1.90×10^{-2}	5.06×10^{-2}
	Closed volume	1.42×10^{-2}	2.82×10^{-2}	4.24×10^{-2}

Table 3. Enthalpies of reaction (3) ($T = 450$–520 K)

Experiment	$\Delta_r H_T^\circ$ (3), kJ/mol		
	$Zn(C_6F_5)^+$	$ZnF(C_6F_5)^+$	$Zn(C_6F_5)_2^+$
1	438.9 ± 1.4	423.0 ± 1.9	435.9 ± 4.1
2	426.3 ± 3.1	426.9 ± 3.3	410.4 ± 3.8
3	420.0 ± 2.9	420.0 ± 3.9	418.8 ± 3.5
Average	428.4 ± 9.7	423.3 ± 4.6	421.7 ± 13.5

that the dissociative ionization of pentafluorodiphenylzinc proceeds via the reaction

$$Zn(C_6F_5)_2 + \bar{e} = Zn^+ + 2C_6F_5^\bullet + 2\bar{e},$$

and using the known values of standard enthalpies of formation of the zinc ion ($\Delta_f H_{298}^\circ(Zn^+) = 1043.1 \pm 0.25$ kJ/mol [41]) and pentafluorophenyl radical ($\Delta_f H_{298}^\circ\left(C_6F_5^\bullet\right) = -547.7 \pm 8.4$ kJ/mol [42]), we found the upper limit of the enthalpy of formation of pentafluorodiphenylzinc in the gas phase: $\Delta_f H_{298}^\circ(Zn(C_6F_5)_2, g) \le -1422.6 \pm 31.3$ kJ/mol. Based on this value, the enthalpy of reaction (3), and the standard enthalpy of formation of carbon dioxide ($\Delta_f H_{298}^\circ(CO_2) = -393.5 \pm 0.4$ kJ/mol [43]), we estimated the standard enthalpy of formation of crystalline zinc pentafluorobenzoate: $\Delta_f H_{298}^\circ \le -2634.1 \pm 32.2$ kJ/mol.

The vaporization of silver pentafluorobenzoate in a temperature range of 370–461 K was shown previously [44] to be accompanied by the complete thermal decomposition of the complex with the formation of metallic silver and transition to the gas phase of pentafluorodiphenyl $C_{12}F_{10}$ and carbon dioxide CO_2 molecules. A similar mechanism of the thermal behavior of this complex is characteristic of nearly all silver compounds due to a low energy of the metal–ligand bond. As should be expected, the zinc complex decomposed in a different manner, and the sublimation and decarboxylation of pentafluorobenzoate are accompanied by the formation of pentafluorodiphenylzinc for which the metal–ligand bond energy is much higher than that for the silver complexes. Taking into account the aforesaid, we can expect that the vaporization of the trivalent metal complexes should be accompanied by the formation of pentafluorotriphenyl compounds in the gas phase, and the possibility of forming pentafluorotetraphenyl complexes of tetravalent metals cannot be excluded in the absence of serious steric hindrances.

Dimethyl- [45] or diethylzinc [46, 47] combined with an oxygen source is a widely abundant precursor for the production of zinc oxide by the CVD method. It is very difficult to work with organozinc compounds, because they are unstable in air and vigorously react with water. The studied complex, zinc pentafluorobenzoate, is stable, rather volatile, and transits to the gas phase as one compound, which makes it possible to recommend it as a precursor in the CVD method for the preparation of zinc oxide films in an oxygen atmosphere. The formation of zinc oxide films doped with fluorine can be expected with a high probability, but the synthesis of the material of a specified composition would require further studies.

ACKNOWLEDGMENTS

IR spectroscopy and XRD, phase XRD, and C,H,N,S elemental analyses were carried out using the equipment of the Center for Collective Use "Physical Investigation Methods" at the Kurnakov Institute of the General and Inorganic Chemistry (Russian Academy of Sciences) functioning in terms of state assignment of the Kurnakov Institute of the General and Inorganic Chemistry (Russian Academy of Sciences) in the area of basic research.

FUNDING

This work was supported by the Russian Science Foundation, project no. 21-13-00086.

CONFLICT OF INTEREST

The authors declare that they have no conflicts of interest.

REFERENCES

1. Mishra, S. and Daniele, S., *Chem. Rev.*, 2015, vol. 115, p. 8379.
2. Gulino, A., Lupo, F., and Fragala, M.E., *J. Phys. Chem. C*, 2008, vol. 112, p. 13869.
3. Gulino, A., Castelli, F., Dapporto, P., et al., *Chem. Mater.*, 2000, vol. 12, p. 548.
4. Wasim, M., Shi, F., Liu, J., et al., *J. Polym. Res.*, 2021, vol. 28, p. 338.
5. Hu, J. and Gordon, R.G., *Solar Cells*, 1991, vol. 30, p. 437.
6. Choi, B.G., Kim, I.H., Kim, D.H., et al., *J. Eur. Ceram. Soc.*, 2005, vol. 25, p. 2161.
7. Hong, R.Y., Li, J.H., Chen, L.L., et al., *Powder Technol.*, 2009, vol. 189, p. 426.
8. Huang, J.R., Wu, Y.J., Gu, C.P., et al., *Sens. Actuat.*, 2010, vol. 146, p. 206.
9. Xuan, J., Zhao, G., Sun, M., et al., *RSC Adv.*, 2020, vol. 10, p. 39786.
10. Wolska-Pietkiewicz, M., Tokarska, K., Wojewodzka, A., et al., *Sci. Rep.*, 2019, vol. 9, p. 18071.
11. Applerot, G., Lipovsky, A., and Dror, R., *Adv. Funct. Mater.*, 2009, vol. 19, p. 842.
12. Kityk, I., Migalska-Zalas, A., Ebothe, J., et al., *Cryst. Res. Technol.*, 2002, vol. 37, p. 340.
13. El Hichou, A., Bougrine, A., Budendorff, J.L., et al., *Semicond. Sci. Technol.*, 2002, vol. 17, p. 607.
14. Najafi, N. and Rozati, S.M., *J. Elec. Mater.*, 2018, vol. 47, p. 1962.
15. Cosham, S.D., Kociok-Kohn, G., Johnson, A.L., et al., *Eur. J. Inorg. Chem.*, 2015, vol. 26, p. 4362.
16. Mahon, M.F., Molloy, K.C., Stanley, J.E., et al., *Appl. Organomet. Chem.*, 2005, vol. 19, p. 658.
17. Johnson, A.L., Kingsley, A.J., Kociok-Köhn, G., et al., *Inorg. Chem.*, 2013, vol. 52, p. 5515.
18. Shmelev, M.A., Voronina, Yu.K., Gogoleva, N.V., et al., *Russ. J. Coord. Chem.*, 2022, vol. 48, no. 4, p. 224.
19. *SMART (control) and SAINT (integration). Software. Version 5.0*, Madison: Bruker AXS Inc., 1997.
20. Sheldrick, G.M., *SADABS*, Madison: Bruker AXS Inc., 1997.
21. Sheldrick, G.M., *Acta Crystallogr., Sect. C: Struct. Chem.*, 2015, vol. 71, p. 3.
22. Dolomanov, O.V., Bourhis, L.J., Gildea, R.J., et al., *J. Appl. Crystallogr.*, 2009, vol. 42, p. 339.
23. Alvarez, S. and Llunell, M., *Dalton Trans.*, 2000, no. 19, p. 3288.
24. Casanova, D., Llunell, M., Alemany, P., and Alvarez, S., *Chem.-Eur. J.*, 2005, vol. 11, p. 1479.
25. Shmelev, M.A., Gogoleva, N.V., Kuznetsova, G.N., et al., *Russ. J. Coord. Chem.*, 2020, vol. 46, no. 8, p. 557. https://doi.org/10.1134/S1070328420080060
26. Shmelev, M.A., Kiskin, M.A., Voronina, J.K., et al., *Materials*, 2020, vol. 13, no. 5689.
27. Walsh, J.P.S., Sproules, S., Chilton, N.F., et al., *Inorg. Chem.*, 2014, vol. 53, p. 8464.
28. Zampakou, M., Rizeq, N., Tangoulis, V., et al., *Inorg. Chem.*, 2014, vol. 53, p. 2040.
29. Karmakar, A., Sarma, R.J., and Baruah, J.B., *Eur. J. Inorg. Chem.*, 2007, p. 643.
30. Cai, W.-X., *Z. Kristallogr. NCS*, 2007, vol. 222, p. 217.
31. Boyle, T.J., Raymond, R., Boye, D.M., et al., *Dalton Trans.*, 2010, vol. 39, p. 8050.
32. Roy, S., Bauza, A., Frontera, A., et al., *Inorg. Chim. Acta*, 2015, vol. 440, p. 38.
33. Zhao, G.-L. and Wen, Y.-H., *Acta Crystallogr., Sect. E: Struct. Rep. Online*, 2005, vol. 61, p. m2699.
34. Karmakar, A., Baruah, J.B., et al., *Polyhedron*, 2008, vol. 27, p. 3409.
35. Karmakar, A., Bania, K., Baruah, A.M., et al., *Inorg. Chem. Commun.*, 2007, vol. 10, p. 959.
36. Dey, D., Roy, S., Purkayastha, R.N.D., et al., *J. Coord. Chem.*, 2011, vol. 64, no. 7, p. 1165.
37. Singh, B., Long, J.R., de Biani, F.F., et al., *J. Am. Chem. Soc.*, 1997, vol. 119, p. 7030.
38. Shmelev, M.A., Kuznetsova, G.N., Dolgushin, F.M., et al., *Russ. J. Coord. Chem.*, 2021, vol. 47, no. 2, p. 127. https://doi.org/10.1134/S1070328421020068
39. Gribchenkova, N.A. and Alikhanyan, A.S., *J. Alloys Compd.*, 2019, vol. 778, p. 77.
40. Gurvich, L.V., Karachentsev, G.V., Kondrat'ev, V.N., et al., *Energii razryva khimicheskikh svyazei. Potentsialy ionizatsii i srodstvo k elektronu* (Chemical Bond Energies. Ionization Potentials and Electron Affinities), Moscow: Nauka, 1974.
41. *Termicheskie konstanty veshchestv. Spravochnik* (Thermal Parameters of Compounds. Handbook), Glushko, V.P., Ed., Moscow: VINITI, 1973, vol. VI, ch. 2.
42. Yu-Ran Luo., *Handbook of Bond Energies in Organic Compounds*, CRC Press, 2003.
43. *Termicheskie konstanty veshchestv. Spravochnik* (Thermal Parameters of Compounds. Handbook), Glushko, V.P., Ed., Moscow: VINITI, 1971, vol. IV, ch. 2.
44. Malkerova, I.P., Kayumova, D.B., Belova, E.V., et al., Russ. *J. Coord. Chem.*, 2022, vol. 48, no. 2, p. 84. https://doi.org/10.1134/S107032842202004X
45. Black, K., Jones, A.C., Alexandrou, I., et al., *Nanotecnology*, 2010, vol. 21, p. 045701.
46. Wieldraaijer, W., Van Balen Blanken, J., and Kuiopers, E.W., *J. Cryst. Growt*h., 1993, vol. 126, p. 305.
47. Alessandri, I., Zucca, M., Ferroni, M., et al., *Cryst. Growth Des.*, 2009, vol. 9, p. 1258.

Translated by E. Yablonskaya